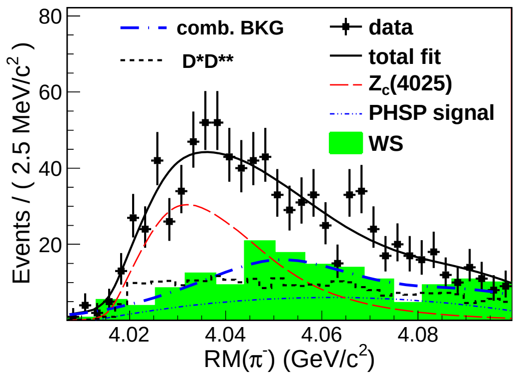


FIG. 4. Unbinned maximum likelihood fit to the $\pi^-$ recoil mass spectrum in data. See the text for a detailed description of the various components that are used in the fit. The scale of the $D^*D^{**}$ shape is arbitrary.

$p \cdot q$

$$\left|\frac{1}{M^2 - m^2 + im\Gamma/c^2}\right|^2 \cdot p \cdot q. \qquad (1)$$

Here, $M$ is the reconstructed mass; $m$ is the resonance mass; $\Gamma$ is the width; $p(q)$ is the $D^{*+}(\pi^-)$ momentum in the rest frame of the $D^{*+}\bar{D}^{*0}$ system (the initial $e^+e^-$ system).

The signal yield of the $Z_c^+(4025)$ is estimated by an unbinned maximum likelihood fit to the spectrum of $RM(\pi^-)$. The fit results are shown in Fig. 4. Possible interference between the $Z_c^+(4025)$ signals and the PHSP processes is neglected. The $Z_c^+(4025)$ signal shape is taken as an efficiency-weighted BW shape convoluted with a detector resolution function, which is obtained from MC simulation. The detector resolution is about $2\,\mathrm{MeV}/c^2$ and is asymmetric due to the effects of ISR. The shape of the combinatorial backgrounds is taken from the kernel-estimate [21] of the WS events and its magnitude is fixed to the number of the fitted background events within the signal window in Fig. 3(a). The shape of the PHSP signal is taken from the MC simulation and its amplitude is taken as a free parameter in the fit. By using the MC shape, the smearing due to effects of ISR and the detector resolution are taken into account. From the fit, the parameters of $m$ and $\Gamma$ in Eq. (1) are determined to be

$$m(Z_c^+(4025)) = (4026.3 \pm 2.6)\,\mathrm{MeV}/c^2,$$
$$\Gamma(Z_c^+(4025)) = (24.8 \pm 5.6)\,\mathrm{MeV}.$$

A goodness-of-fit test gives a $\chi^2/\mathrm{d.o.f.} = 30.4/33 = 0.92$. The $Z_c^+(4025)$ signal is observed with a statistical significance of $13\,\sigma$, as determined by the ratio of the maximum likelihood value and the likelihood value for a fit with a null-signal hypothesis. When the systematic uncertainties are taken into account, the significance is evaluated to be $10\,\sigma$.

The Born cross section is determined from $\sigma = \frac{n_{\mathrm{sig}}}{\mathcal{L}(1+\delta)\varepsilon\mathcal{B}}$, where $n_{\mathrm{sig}}$ is the number of observed signal events, $\mathcal{L}$ is the integrated luminosity, $\varepsilon$ is the detection efficiency, $1+\delta$ is the radiative correction factor and $\mathcal{B}$ is the branching fraction of $D^{*+} \to D^+(\pi^0, \gamma)$, $D^+ \to K^-\pi^+\pi^+$. From the fit results, we obtain $560.1 \pm 30.6$ $D^{*+}\bar{D}^{*0}\pi^-$ events, among which $400.9 \pm 47.3$ events are $Z_c^+(4025)$ candidates. With the input of the observed center-of-mass energy dependence of $\sigma(D^{*+}\bar{D}^{*0}\pi^-)$, the radiative correction factor is calculated to second-order in QED [22] to be $0.78 \pm 0.03$. The efficiency for the $Z_c^+(4025)$ signal process is determined to be 23.5%, while the efficiency of the PHSP signal process is 17.4%. The total cross section $\sigma(e^+e^- \to (D^*\bar{D}^*)^{\mp}\pi^{\pm})$ is measured to be $(137 \pm 9)\,\mathrm{pb}$, and the ratio $R = \frac{\sigma(e^+e^- \to Z_c^{\pm}(4025)\pi^{\mp} \to (D^*\bar{D}^*)^{\pm}\pi^{\mp})}{\sigma(e^+e^- \to (D^*\bar{D}^*)^{\pm}\pi^{\mp})}$ is determined to be $0.65 \pm 0.09$.

| Source | $m$(MeV/$c^2$) | $\Gamma$(MeV) | $\sigma_{\mathrm{tot}}$(%) | $R$(%) |
|---|---|---|---|---|
| Tracking | | | 4 | |
| Particle ID | | | 5 | |
| Tagging $\pi^0$ | | | 4 | |
| Mass scale | 1.8 | | | |
| Signal shape | 1.4 | 7.3 | 1 | 5 |
| Backgrounds | 1.5 | 0.6 | 5 | 5 |
| Efficiencies | 0.9 | 2.2 | 1 | 5 |
| $D^{**}$ states | 2.2 | 0.7 | 5 | 2 |
| Fit range | 0.9 | 0.9 | 1 | 1 |
| $D^{*+}\bar{D}^{*0}\pi^-$ line shape | | | 4 | |
| PHSP model | | | 2 | 2 |
| Luminosity | | | 1.0 | |
| Branching fractions | | | 2.6 | |
| total | 3.7 | 7.7 | 11 | 9 |

TABLE I. A summary of the systematic uncertainties on the measurements of the $Z_c^+(4025)$ resonance parameters and cross sections. We denote $\sigma_{\mathrm{tot}} = \sigma(e^+e^- \to (D^*\bar{D}^*)^{\pm}\pi^{\mp})$. The total systematic uncertainty is taken as the square root of the quadratic sum of the individual uncertainties.

Sources of systematic error on the measurement of the $Z_c^+(4025)$ resonance parameters and the cross section are listed in Table I. The main sources of systematic uncertainties relevant for determining the $Z_c^+(4025)$ resonance parameters and the ratio $R$ include the mass scale, the signal shape, background models and potential $D^{**}$ backgrounds. We use the process $e^+e^- \to D^+\bar{D}^{*0}\pi^-$ to study the mass scale of the recoil mass of the low momentum bachelor $\pi^-$. By fitting the peak of $\bar{D}^{*0}$ in the $D^+\pi^-$ recoil mass spectrum, we obtain a mass of $2008.6 \pm 0.1\,\mathrm{MeV}/c^2$. This deviates from the PDG reference value by $1.6 \pm 0.2\,\mathrm{MeV}/c^2$. Since the fitted variable $RM(D^+\pi^-) + M(D^+) - m(D^+)$ removes the correlation with $M(D^+)$, the shift mostly is due to the momentum measurement of the bachelor $\pi^-$. Hence, we take the mass shift of $1.8\,\mathrm{MeV}/c^2$ as a systematic uncertainty on $RM(\pi^-)$ due to the mass scale. If one assumes $Z_c^+(4025)$ also decays to other final states such as $\pi^+(\psi(2S), J/\psi, h_c)$, variations of their relative coupling strengths would affect the measurements of the $Z_c^+(4025)$ mass and width. The Flatté formula [23] is used to take into account possible multiple channels, and the maximum changes on the mass and the width are $0.4\,\mathrm{MeV}/c^2$ and $0.1\,\mathrm{MeV}$, respectively. When we as-